Electron states of interface iron silicides on Si(111)7×7

Fausto Sirotti
Laboratoire pour l'Utilisation du Rayonnement Electromagnetique, Centre National de la Recherche Scientifique-Commissariat à l'Énergie Atomique Universite de Paris–Sud, F-91405 Orsay, France
and Laboratorium fur Festkoerperphysik, Eidgenössische Technische Hochschule, CH-8093 Zurich, Switzerland

Maurizio DeSantis*
Laboratoire pour l'Utilisation du Rayonnement Electromagnetique, Centre National de la Recherche Scientifique-Commissariat à l'Énergie Atomique Universite de Paris–Sud, F-91405 Orsay, France
and Dipartimento di Fisica dell Universita dell'Aquila, Italy

Xiaofeng Jin
Laboratoire pour l'Utilisation du Rayonnement Electromagnetique, Centre National de la Recherche Scientifique-Commissariat à l'Énergie Atomique Universite de Paris–Sud, F-91405 Orsay, France
and Physics Department, Fudan University, Shanghai, People's Republic of China

Giorgio Rossi
Laboratoire pour l'Utilisation du Rayonnement Electromagnetique, Centre National de la Recherche Scientifique-Commissariat à l'Énergie Atomique Universite de Paris–Sud, F-91405 Orsay, France
and Laboratorium fur Festkoerperphysik, Eidgenössische Technische Hochschule, CH-8093 Zurich, Switzerland
(Received 18 October 1993; revised manuscript received 16 December 1993)

Solid-phase epitaxy of iron silicides on Si(111)7×7 substrates is studied by comparing photoemission spectroscopy of the extended states and core levels, and Fe $L_{2,3}$ x-ray-absorption spectroscopy, for the interface phases and the bulk stoichiometric silicides. Epitaxial growth favors the low-temperature formation of metallic tetragonal α-$FeSi_2$ which starts decomposing irreversibly into semiconducting orthorhombic β-$FeSi_2$ at above 600 °C. This interface chemistry is opposite to the bulk phase diagram where the α phase is the high-temperature stable disilicide which reversibly transforms into the β phase when the temperature is lowered to 950 °C. No evidence of metastable interface phases other than the bulk phases is found. The coexistence of bulk epitaxial phases over an extended temperature range indicates that local properties of the interface strongly influence the silicide phase transitions.

INTRODUCTION

The growth of crystallographically and chemically ordered metastable phases on surfaces is one of the avenues opened by surface science to nanotechnology. In the case of epitaxy on semiconductors, the main goals are the growth of monolithic junctions with low-defect layers of insulating, semiconducting, metallic, and perhaps ferromagnetic materials. Semiconductor heterojunctions have been developed mostly on III-V group and II-VI group semiconductors, while Schottky barriers with metallic silicides are at the basis of silicon technology. The Si(111) surface supports the epitaxy of single-crystal layers of metallic silicides in the CaF_2 structure, like $CoSi_2$ and $NiSi_2$, as well as of insulating calcium-fluorite layers.[1] Epitaxial overgrowth of silicon on top of the silicides has also been clearly demonstrated[2] and applied to form metal-based transistor structures. Starting in the early 90s interest grew in exploring the possibility of growing epitaxially on silicon a direct-gap semiconductor, still in the form of a silicide, like the β phase of $FeSi_2$, or $CrSi_2$.[3] Furthermore, theoretical predictions[4] of a bulk instable allotropic phase of $FeSi_2$ with CaF_2-type structure, and the silicon lattice parameter, with its metallic character stabilized by ferromagnetic exchange, prompted a large research effort in the Si-Fe interface structure and the growth techniques for such a metastable phase.[5,6] A rich literature now exists for the silicon-iron-silicide system: the epitaxy of the semiconducting β phase has been characterized as a three-domain growth of the orthorhombic β-phase lattice with β-$FeSi_2$(101):Si(111) or β-$FeSi_2$(110):Si(111).[7] The large density of structural defects for this interface (domains) has frustrated applications of this system to the development and infrared detectors of all-silicon technology. Evidence of a cubic silicide with a CsCl-type lattice, and stoichiometries ranging from FeSi almost to $FeSi_2$ have also been obtained,[8] showing the real possibility of growing lattice-matched metastable phases of iron silicides on the Si(111) surface. Finally, some evidence of a truly CaF_2-type γ phase of iron disilicide has been obtained[9] by growing the silicide layer by molecular-beam epitaxy (MBE) within a rather narrow domain of growth-parameter space (thickness, temperature, and codeposition). These metastable phases convert to the (agglomerated) semiconducting β-$FeSi_2$ phase for annealing temperatures above 600 °C. The cubic phases of CsCl- or CaF_2-type structures are metallic, but no clear evidence of magnetism has been ob-

tained. One should note here that Fe-Si amorphous alloys are ferromagnetic for a wide variety of composition, and are employed in technology.

The metallic character of the interface phases is also a property of the high-temperature stable bulk iron disilicide phase, the α-$FeSi_2$ phase which decomposes to the β phase below 950 °C (Ref. 10) but can be quenched to a metastable low-temperature state. The α phase has a tetragonal structure which is in fact very similar to the interface metastable CsCl phase of FeSi: it can be obtained from this by removing every second Fe plane. Little attention has been given to this phase until very recently when the α phase was grown by MBE onto Si(111) at low temperature.[11]

The studies of the type of iron silicide epitaxy on silicon has been carried mostly out by surface crystallography techniques [reflection high-energy electron diffraction (RHEED),[5,8,11] low-energy electron diffraction (LEED),[12] scanning tunneling microscopy (STM),[5,13] x-ray diffraction,[7,11,14] and surface-extended x-ray-absorption fine structure (SEXAFS) (Ref. 15)] and by electron microscopy,[1] with the spectroscopy work mostly limited to establishing the near-surface composition (Auger[16] and x-ray photoemission[17]) and the metallic density of states of the extended electron bands (ultraviolet photoemission).[18] However, a direct probe of the electron states is the ultimate test for recognizing the properties of the interface silicides which can differ, even for a given crystallographic phase, as a function of the compositional order, defects, or distortions due to epitaxial strain. We therefore carried out, prior to the present work, a careful study of the occupied and unoccupied electron states of the stable iron silicides in the composition range relevant to epitaxial growth, by photoemission and x-ray absorption with synchrotron radiation. The photoemission line-shape analysis of the Fe and Si core levels are determined by metallic screening, exchange splitting, and surface shifts of the terminating layers. These results are collected in Ref. 19, and provide the basis for the discussion of the interface phases presented here which were studied by core-level photoemission data for Fe 3*s* and 3*p*, and Si 2*p* along with valence bands, Si Auger *LVV* line shapes, and Fe $L_{2,3}$ x-ray-absorption edges as a function of thickness of the interface silicide and thermal treatment. Two approaches have been followed in the literature for the growth of iron silicides on Si(111): the codeposition in stoichiometric proportions of Fe and Si, i.e., the MBE method, and the solid-state reaction between the silicon substrate and an ultrathin layer of Fe deposited at low temperature and then annealed, or solid-phase-epitaxy (SPE) method. The main difference between the two approaches is that in MBE the substrate provides only the bond ordering at the interface, and the overlayer can grow on this template without extensive mass transport. SPE, on the contrary, starts with the chemisorption of iron on surface sites and only as a function of the buildup of the chemical potential of the overlayer, and/or of the thermally promoted mobility of the substrate atoms, interdiffusion, and simultaneous registry of the nucleated silicide may occur. SPE is therefore a surface destructive technique, unlike MBE, but is better suited if one is interested in studying the evolution toward equilibrium of a solid perturbed by the adsorption of foreign atoms, since all the interface thermodynamics, including mass transport through the interface, is at work in this case. Our choice here is to adopt the SPE technique to study the interface formation between iron and silicon when ultrathin layers of iron are deposited and allowed to react by thermal annealing with a semi-infinite single crystal of silicon through a temperature range that spans the formation temperature of the stable silicide compounds.

We will concentrate our analysis on Fe coverages of 1.5×10^{15} and 3×10^{15} atoms cm^{-2}. These two deposits on the Si(111)7×7 surface would lead to thicknesses, respectively, of two and four monolayers of pure iron in the absence of intermixing, with the customary definition of a monolayer based on the surface concentration (atoms/cm^2) of the substrate.

The choice is dictated by the goal of studying the formation of interface-stable silicides in the ultrathin regime, but well above the surface chemisorption regime which is only a precursor to interface formation: the arrangement of submonolayer amounts of Fe is dictated by chemisorption on surface sites[6,20] and cannot uniquely indicate the silicide structure. The bulk densities of the disilicides are 4.75 g cm^{-3} for the ideally matched γ phase, 4.99 g cm^{-3} for the α phase, and 4.94 g cm^{-3} for the β phase. It follows that the two Fe coverages, when fully reacted to a disilicide covering the silicon surface, will produce a silicide thickness of 5.5–6 and 11–12 Å depending on the phase.

EXPERIMENT

Sample preparation and measurements were done in an ultrahigh-vacuum apparatus with a base pressure of 1×10^{-10} mbar equipped with a cylindrical-type electrostatic energy analyzer (MAC-II Riber) and standard surface science facilities. The experiments were done at LURE-Orsay using the SU7-beam line of the SuperAco positron storage ring. Undulator radiation linearly polarized in the horizontal plane was monochromatized by a 10-m toroidal grating monochromator in the range 130–900 eV with a resolving power of 10^3, and focused onto the sample surface. The geometry of the experiment was identical to that described in Ref. 19. The overall experimental resolution in the photoemission spectra is 350 meV, as checked by the Fermi level of an atomically clean polycrystalline Cu sample. The total electron yield ejected as a consequence of x-ray absorption was collected by an electron multiplier followed by a digital picoamperometer, as well as directly by a picoamperometer measuring the sample current. In the Fe $L_{2,3}$-edge absorption measurements the sample normal was oriented at 45° with respect to the polarization of the x rays. The Si(111)7×7 surfaces were prepared from P-doped wafers by cycles of Ar-ion bombardment, flash annealing at 1150 °C, and subsequent slow cooling until sharp 7×7 LEED patterns were observed. Fe was deposited onto silicon from electron-beam-heated rods of 99.999 nominal purity (main impurity: silicon, 5 ppm in weight). The

deposition rate was controlled by a quartz microbalance mounted on the manipulator opposite to the samples, in order to see the Fe source under the same solid angle when oriented to the evaporator. The rate was set at 0.2 monolayers (ML)/min in a vacuum never exceeding 8×10^{-10} mbar, and the sample expositions were timed. A conservative error bar on the absolute coverages is ±20%, while relative coverages are accurate, as also confirmed by Auger spectroscopy. Annealing of the interfaces was performed by passing a dc current through the silicon wafer substrate. This could be done at any position of the sample including the spectroscopic measurement position.

RESULTS AND DISCUSSION

The solid-phase epitaxy of the interface silicides was followed at discrete annealing stages by electron spectroscopy and LEED pattern observations. The average composition of the top 10–15 Å of material is deduced from the intensity ratio (peak areas) of representative peaks of iron and silicon. The diagram of Fig. 1 presents the results for the growth of interface silicides as a function of the abundance of Fe at the initial surface, and as a function of annealing temperature. The deposition of 1.5×10^{15} Fe atoms/cm^2 produces a disordered intermixed phase at room temperature, an interface silicide of average composition approximately 1:1.7 displaying a 1×1 LEED pattern after the first annealing step at 200 °C, and a disilicide after annealing at about 300 °C with a total thickness of 5–6 Å and a 2×2 LEED pattern. The deposit of 3×10^{15} Fe atoms/cm^2 produces a disordered Fe-rich intermixed phase at room temperature, an intermediate 1×1-ordered silicide after annealing at 250 °C and a disilicide after annealing at 450 °C, with a total thickness of 11–12 Å and a 2×2 LEED pattern. At temperatures higher than 500 °C agglomeration of the silicide takes place, and increasingly large portions of the substrate are uncovered. At 750 °C the uncovered silicon substrate reconstructs to give the 7×7 LEED pattern. Apart from a difference in the kinetics of the interface silicide formation, which can be attributed to mass transport across the first epitaxial silicide layer, no other major differences occur between the two coverages discussed here. The spectroscopy results will therefore be discussed mostly for the thicker sample in order to reduce the weight of substrate contribution in the silicon line-shape analysis.

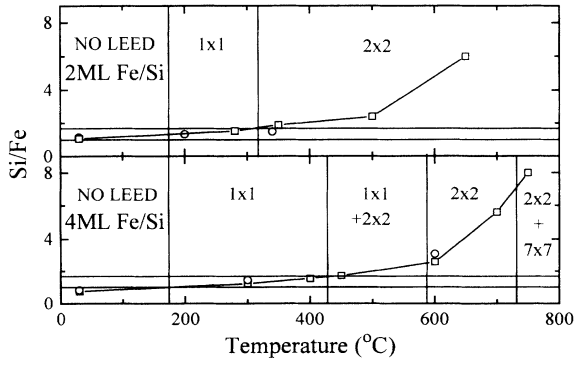

FIG. 1. Intensity ratios between the Auger Si LVV and the Fe 3*p* photoemission peaks as a function of thermal treatment for two representative Fe deposits: 1.5×10^{15} and 3×10^{15} Fe atoms/cm^2 equivalent to two and four Fe atomic planes (monolayers) at the Si(111) surface concentration (7.8×10^{14} atoms/cm^2). The two horizontal lines represent the ratio measured for bulk ε-FeSi and for α-$FeSi_2$ and β-$FeSi_2$. The LEED patterns observed are also indicated.

Interface growth for 3×10^{15} Fe atoms/cm^2 on Si(111)7×7

Occupied electron states

The valence-band spectra at the relevant steps of the interface growth are summarized in Fig. 2. The photon energy of $h\nu=170$ eV favors the photoemission from the Fe 3*d* bands with respect to the Si 3*p* bands by a factor 30, due to the relative value of photoionization cross sections.[21] The spectra are therefore normalized for graphical reasons. The as-deposited interface presents a high density of states at the Fermi level, a peak located at −0.5 eV, and a shoulder at −1.5 eV. After the first thermal treatment at 300 °C the line shape changes drastically. The peak becomes more symmetric with the maximum at 0.75 eV. This line shape is little affected by annealing at 400 °C, but the maximum of the density of states (DOS) moves to 0.85 eV. This line shape remains unchanged for the following annealing at 450 and 500 °C. At 600 °C two shoulders appear at −0.3 and at about −2.3 eV. These features are more evident after annealing at 650 and 750 °C. The energy distribution curve (EDC) of pure Si(111)7×7 is also given for comparison. The density of states at the Fermi level always shows an edge which becomes weak at high annealing temperatures but is distinctly different from the tail of states at the

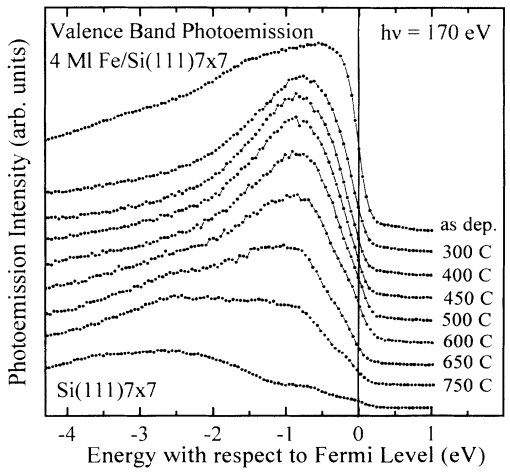

FIG. 2. Valence-band electron energy distribution curves obtained with $h\nu=170$ eV excitation from the 4-ML Fe/Si(111) interface after the most relevant thermal treatments. The valence band of Si(111)7×7 clean surface is also shown for comparison. The intensities are multiplied by different values to facilitate the comparison of line shapes.

valence-band maximum of a semiconductor. The Si(111)7×7 spectrum also shows a metallic edge due to the adatom bands. From this result one must therefore conclude that a metallic phase is always present at the interface, although it becomes a minority phase for annealing temperatures exceeding 600 °C. The Fe 3*d* states dominate the spectra up to 650 °C, but peaks of the Si 3*p* partial density of states are clearly distinguished for annealings higher than 600 °C. Due to the relative photoionization cross section, this fact indicates that the iron silicides become a minority species in the near surface region at temperatures of 650 °C and higher, as also seen in the Si/Fe ratio of Fig. 1. The coexistence of silicon-derived valence-band peaks with Fe 3*d*-derived peaks, as well as the coexistence of two LEED patterns after annealing at 750 °C, shows the phase separation of the silicide and silicon substrate.

A comparison of the valence-band spectra with those of bulk silicides is done in Fig. 3. The as-deposited interface (points) is compared to the spectrum of bulk ε-FeSi (continuous line). The two spectra show a similarly high density of 3*d*-derived states, but the details of the density of states are quite different. In particular the peak of the interface is at higher binding energy, and it is less prominent than the peak of the narrow-band semiconductor ε-FeSi. Two FeSi phases have been observed to grow epitaxially on Si(111)7×7: the bulk stable ε-FeSi (Ref. 14) and a CsCl-type simple cubic phase,[8] but the width of the *d* band at the interface rather suggests that a Fe-rich solid solution is formed. The interface silicide stable between 400 and 500 °C is then compared with the spectrum of bulk α-$FeSi_2$ in the central panel of the figure. Here the similarity of the two spectra is striking, and gives a first strong evidence of the nucleation of epitaxial (i.e., weakly strained) α-$FeSi_2$. Finally, in the bottom of Fig. 3, the valence band for the high-temperature-annealed interface (points) is compared with a combination (continuous line) of three contributions: clean Si(111)7×7 from the uncovered reconstructed substrate, metallic α-$FeSi_2$, and semiconducting β-$FeSi_2$. The double edge seen in the interface spectra starting at 600 °C is explained by the coexistence of α-$FeSi_2$ and β-$FeSi_2$ in different proportions at the interface. The metallic states at the Fermi level for the high-temperature-annealed interfaces are therefore due to a heterogeneous surface which contains both semiconducting and metallic silicides, along with the uncovered portions of the substrate. The total 3*d* signal (α-$FeSi_2$ + β-$FeSi_2$ in equal proportions) corresponds to silicide islands covering 30% of the substrate.

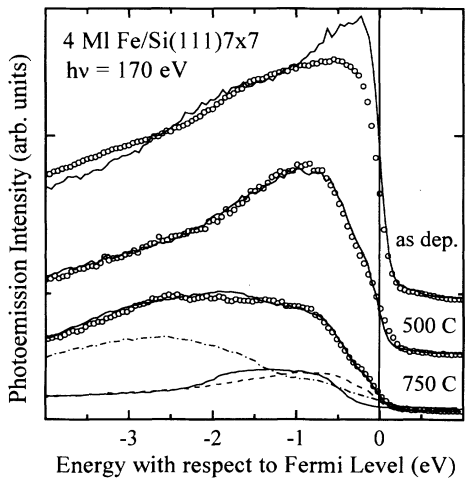

FIG. 3. Comparison between valence-band spectra of the Fe/Si interface (points) and of bulk silicides (continuous lines). The spectrum of the as-deposited sample is compared with that of ε-FeSi. The interface annealed at 500 °C is compared to α-$FeSi_2$. The interface annealed at 750 °C is compared to the sum of the spectra of the clean Si(111)7×7 surface (dot-dashed line), α-$FeSi_2$ (dashed line), and β-$FeSi_2$ (continuous line).

Unoccupied Fe 3d states

The x-ray absorption spectroscopy (XAS) spectra of the Fe 2*p* core level represent the Fe 3*d* empty density of states in the presence of the Fe 2*p* core hole. Selected data (points) are presented in Fig. 4 and compared to the spectra of bulk silicides (continuous lines). The spectrum of the as-deposited interface shows rather symmetric edges, with a branching ratio higher than the statistical value. It is compared to the combination of the spectra obtained from ε-FeSi and bcc Fe. The good agreement of the nonstatistical branching ratio confirms the formation of an iron-rich solid solution. The annealed interface at 300 °C shows an almost statistical branching ratio and broadened line shape. The spectrum for the interface annealed at 600 °C, i.e., in the disilicide regime, shows a rounded peak and strictly statistical branching ratio. Empirically, it is found that the high-spin Fe compounds all have a high branching ratio, while the low-spin Fe compounds have a nearly statistical branching ratio.[22]

The two curves measured after annealing are in reasonable agreement with the spectrum obtained from bulk α-

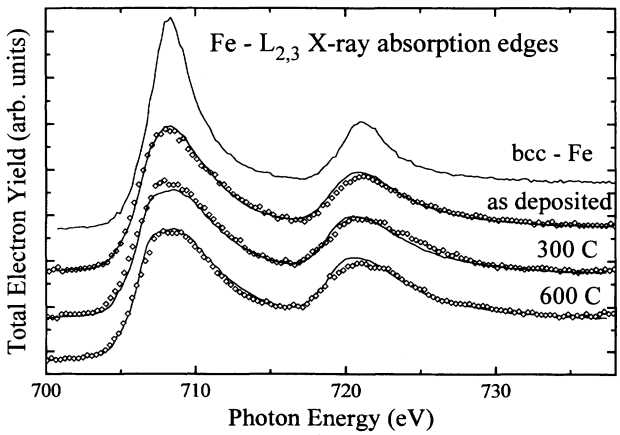

FIG. 4. Fe $L_{2,3}$ x-ray absorption edges of the 4-ML/Si(111) interface at selected annealing steps (points). The as-deposited sample is compared with the sum of the ε-FeSi (70%) and bcc-Fe (30%) reference spectra.

$FeSi_2$, indicating that these interfaces are in fact low-spin compounds.

Core levels

The core-level photoemission spectra were measured with kinetic energies in the interval 70–110 eV, i.e., with high surface sensitivity (an escape depth of 7–10 Å). The Fe spectra are compared to the line shapes of bulk silicides, or to combinations of silicide line shapes, while the Si 2*p* spectra are deconvoluted with components due to various environments of the Si atoms.

Fe 3p

The Fe 3*p* core levels are collected in Fig. 5 for selected annealing temperatures (points). The top curve is measured on the as-deposited interface: it presents a peak at 52.8-eV binding energy, and an intense tail. After annealing at 300 °C, the peak shifts to 53.2 eV and the lineshape becomes less asymmetric. For annealings at temperatures between 400 and 500 °C the Fe 3*p* line shape is stable, peaked at 53.3 eV. After annealing at 600 °C, the photoemission 3*p* peak is displaced to 53.5 eV and strongly broadened. The interface data points are compared to the Fe 3*p* line shapes measured for bulk silicides in strictly identical experimental conditions, and kinetic energies (continuous lines).[19] The comparison provides an important criterion for the assessment of the Fe environment at the interface. Core-level binding energies and line shapes

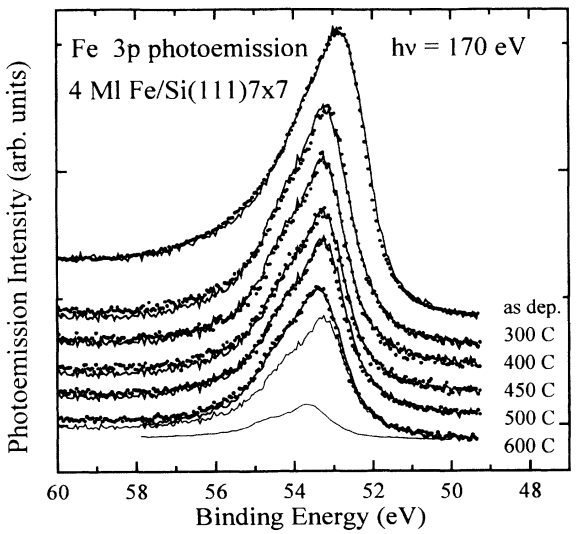

FIG. 5. Fe 3*p* core-level photoemission spectra as measured with $h\nu = 170$ eV on the 4-ML Fe/Si(111) interface (points) compared to the spectra of bulk silicides (continuous lines). The as-deposited interface is compared to the sum of the spectra of ε-FeSi (70%) and bcc Fe (30%). The spectrum of the interface annealed at 300 °C is compared to the sum of the ε-FeSi (30%) and α-$FeSi_2$ (70%) line shapes. The spectra of the interface annealed at 400, 450, and 500 °C are compared to the spectrum of α-$FeSi_2$. The interface spectrum after annealing at 600 °C is compared to the sum of the α-$FeSi_2$ (80%) and β-$FeSi_2$ (20%) line shapes (also shown at the bottom).

are sensitive both to the local structure (number and type of nearest neighbors, interatomic distances) and to the extended electronic structure via the screening effects on the apparent binding energy, the energy-loss spectrum in the tail of the peak (Doniach-Sunjic asymmetry),[23] and the exchange interaction between core hole and polarized valence band if the solid is magnetic. A combination of bulk FeSi (70%) and bcc Fe (30%) spectra is shown to match closely the as-deposited interface, consistently with the absorption data analysis. A combination of FeSi (30%) and α-$FeSi_2$ (70%) line shapes is compared to the interface spectrum after annealing at 300 °C: the interface spectrum cannot be approximated with a single silicide environment due to its width, which is larger than any silicide spectrum and therefore indicates the coexistence of more phases rather than the formation of a novel phase. This is compatible with the concentration gradient of the CsCl-type substitutional $FeSi_{2-x}$ phase.[8] By way of contrast, the pure spectrum of the α-$FeSi_2$ phase represents very accurately the interface Fe 3*p* signal for annealings at 400, 450, and 500 °C. Binding energies and line shapes are basically identical; this is strong evidence for a metallic α-$FeSi_2$-like phase that has fully converted the lower interface silicides at the temperature of 400 °C and that is stable up to above 500 °C. A combination of α-$FeSi_2$ (80%) and β-$FeSi_2$ (20%) line shapes is compared to the spectrum of the interface annealed at 600 °C. The accuracy level of this procedure of subtracting experimental spectra, as determined by comparing the squared residuals, is 5% of the total intensity. The introduction of the β-$FeSi_2$ peak is clearly needed to explain the shift of the interface peak to higher binding energies and the anomalously large width. It therefore results that the interface α-$FeSi_2$ layer starts transforming into the β-$FeSi_2$ phase at a temperature of 600 °C.

Fe 3s

The Fe 3*s* core levels are shown for selected annealing steps in Fig. 6, together with the spectra from bulk standards (continuous lines). The bcc Fe 3*s* peak is shown for comparison; it is joined by a fully spin-polarized satellite[24] at 4.5-eV lower kinetic energy in bcc Fe and in most ferromagnetic compounds of iron.[25] The as-deposited interface is compared with a combination of the FeSi and bcc Fe in the same amount used for the Fe 3*p* core level and the $L_{2,3}$ absorption edges. The spectra for the annealed interface clearly do not present any intensity which could be attributed to satellites of the main 3*s* peak. The peak energies are consistent with the evolution of the Fe 3*p* signals discussed above. The rising intensity at about 6 eV higher binding energy is due to the foot of the Si 2*p* photoemission peak whose intensity increases with the annealing temperature. The line shape of Fe 3*s* after annealing at 500 °C compares well with the corresponding line shape for α-$FeSi_2$, which is nonmagnetic. This disfavors the hypothesis of growth of the ferromagnetically stabilized γ-$FeSi_2$, which could have indeed similar binding energies and line shapes, but should show spectroscopic signatures of the exchange interaction

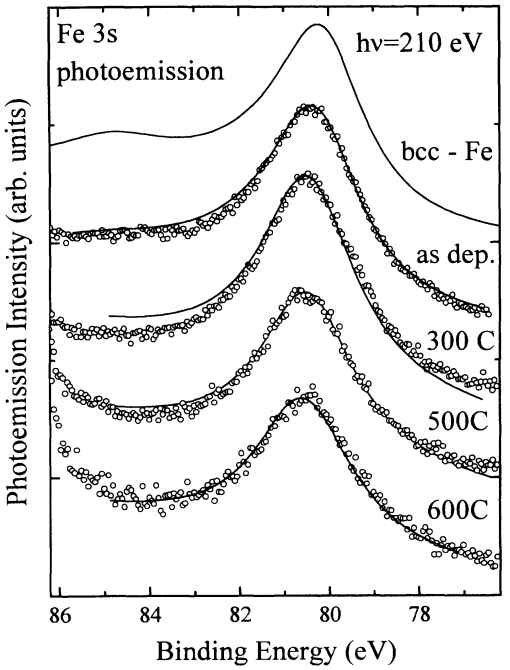

FIG. 6. Fe 3*s* core-level photoemission as measured with $h\nu=210$ eV on the 4-ML Fe/Si(111) interface (points). The continuous lines overlapping the interface spectra represent the line shapes of standard silicides, or line shapes obtained as a sum of silicide spectra. The as-deposited interface is compared with the sum of the ε-FeSi (70%) and bcc-Fe (30%) spectra. The spectrum of the interface annealed at 300 °C is compared to the sum of the FeSi (30%) and α-$FeSi_2$ (70%) spectra. The spectrum of the interface annealed at 500 °C is compared to α-$FeSi_2$. The spectrum of the interface annealed at 600 °C is compared to the sum of the α-$FeSi_2$ (80%) and β-$FeSi_2$ (20%) line shapes.

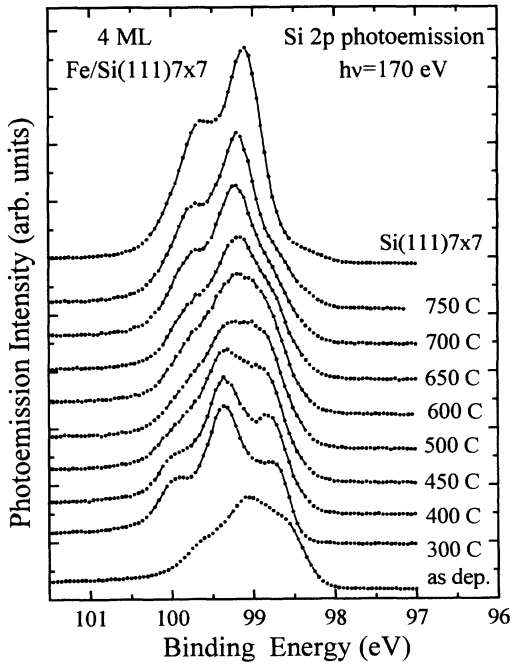

FIG. 7. Si 2*p* core-level spectra as measured with $h\nu=170$ eV of the 4-ML Fe/Si(111) interface after selected thermal treatments. The top curve is the spectrum of the clean Si(111)7×7 surface.

within the Fe 3*d* bands, such as the appearance of the 3*s* core level satellite. After annealing at 600 °C the line shape compares well with the sum of 80% α-$FeSi_2$ and 20% β-$FeSi_2$ line shapes from Ref. 19, in agreement with the Fe 3*p* analysis.

Si 2p

The silicon 2*p* core-level spectra are displayed in Fig. 7, including the reference spectrum for the Si(111)7×7 clean surface. The complexity of the Si signal is clearly seen from the as-deposited interface up to the annealing at 750 °C, where the 7×7-like spectrum again dominates the line shape. This complexity reflects the large variety of atomic sites for Si at the interface, in the silicide(s), at the surface termination of the silicide(s), and in the 2×2 reconstruction which is observed when the α-$FeSi_2$-like phase is formed. To analyze these line shapes unambiguously, an independent criterion is needed: this is provided by the analysis of the Fe 3*p* and 3*s* core levels which have indicated the silicide environment of the Fe atoms. We have therefore decomposed the silicon 2*p* line shapes according to the following criteria: (1) the substrate silicon is represented by the bulk Si doublet obtained by the standard deconvolution of the Si(111)7×7 line shape;[19] (2) the silicon in the silicides is represented by the bulk silicide doublet that was obtained in Ref. 19 by the decomposition of bulk and surface termination peaks for FeSi, α-$FeSi_2$ and β-$FeSi_2$ (all silicides show a surface-shifted Si 2*p* peak at about 0.6-eV lower binding energy, accounting for about 30% of the total intensity as measured at the same kinetic energy as in the present work);[19] and (3) the remaining intensity is fitted by standard doublets and is taken to represent the surface termination and reconstruction of the interface silicide(s), based on the comparison with standards of segregated Si and Fe. This procedure introduces into the first step of analysis of the Si 2*p* line shape the errors connected to the line-shape analysis of the Fe 3*p* (and 3*s* core levels), i.e., the 5% error in the silicide abundancy. The fitting parameters of the bulk silicides are given in Ref. 19, and the binding energies are recalled in Table I. Figure 8 displays the difference curves between the interface samples and the bulk components of the silicides calibrated on the Fe 3*p* core levels. A three-peaked structure is found. This three-peaked line shape is reminiscent of that measured for Si impurities at the surface of Fe polycrystalline films and at the Fe(100) surface, apart from small differences of binding energy to be ascribed to different electronic screening by the substrate, and small variations of the relative intensities. This conclusion is based on a comparison with the spectra independently obtained for surface-segregated Si in Fe, and reported in the bottom of Fig. 8: 8×10^{15} Fe atoms/cm^2 as deposited at room temperature (RT) on Si(111), and the (100) surface of a Fe single crystal containing a bulk concentration of 3% silicon showing segregated Si after prolonged an-

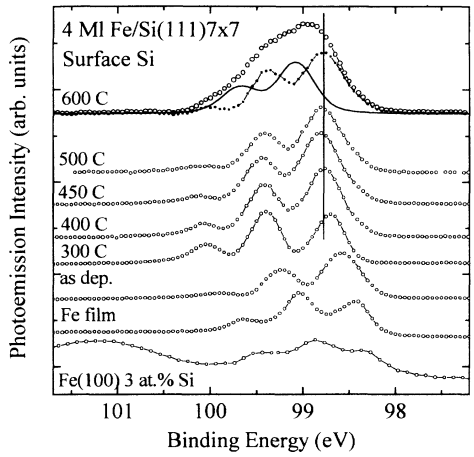

FIG. 8. Surface segregated silicon components of the Si $2p$ core-level line shape measured from the Fe/Si interface. The curves are obtained by subtracting from the spectra of Fig. 7 the bulk component of the silicide spectra of Ref. 19, according to the analysis of the Fe core levels. Two reference spectra are added at the bottom of the figure: segregated Si on Fe(100) 3 at. % Si, and a thick polycrystalline Fe deposit on Si. The peak at 101.3 eV in the Si:Fe(100) spectrum is due to surface-oxidized silicon. It is found that the three-peaked structure of segregated Si is present as a surface component of the interface silicides at all stages of interface reaction. The surface spectrum of the interface after annealing at 600 °C is further deconvoluted, and shows the surface segregated components as well as the bulk Si signal from the uncovered substrate regions that are exposed by the starting agglomeration of the interface silicides (continuous lines). The two vertical bars show the stability of binding energy of the $2p_{3/2}$ peak of segregated silicon, and of the $2p_{1/2}$ peak of adatoms for the annealed interfaces.

TABLE I. Deconvolution results for the Si $2p$ peaks of the 4-ML Fe/Si(111) interface. The silicide binding energies are reported from Ref. 19. The binding-energy values of the surface phases are those of the samples at 500 °C. For all components the scatter of the binding energies at the various thermal treatments of the interface is typically 50 meV. This is also the error bar concerning the possible Schottky-barrier shifts between the interface silicides and the corresponding bulk silicides from Ref. 19. The intensities are quoted as percents of the total intensity measured in each spectrum, i.e., they represent the description of the line shape and should not be compared for different samples. The Si intensity quoted for the interface annealed at 750 °C is the intensity of the total Si(111)7×7 line shape subtracted in the analysis, i.e., it includes the 7×7 surface atoms (see text). The two surface components of the silicides present at the interface annealed at 750 °C are indicated in the "segregated" column, since further decomposition of the adatom intensity is impossible due to overlapping energies.

	Bulk phases				Surface phases	
	FeSi	α-$FeSi_2$	β-$FeSi_2$	Si	Segregated	Adatoms
B.E. (eV)	99.0	99.2	99.7	99.1	98.8	99.5
As deposited	54%				41%	5%
300 °C	20%	40%			25%	15%
400 °C		45%			45%	10%
450 °C		45%			47%	8%
500 °C		45%			47%	8%
600 °C		20%	5%	36%	34%	5%
750 °C		9%	8%	58%	14%+11%	

nealing at 600 °C. The deconvolution of the segregated Si on polycrystalline iron is shown in Fig. 9: the spectrum is accurately fit by two standard doublets with a relative energy shift of 0.57 eV, which indicates that two distinct sites exist for silicon at the iron surface. The three-peaked line shape obtained from the analysis of the interface spectra and shown in Fig. 8 is attributed to the surface silicon termination of the interface iron silicides. Two well-defined bonding configurations exist which we tentatively attribute to segregated island atoms and adatoms. The relative intensity of island and adatom peaks is stable, within the accuracy of our fitting procedure for thermal treatments of the interface above 500 °C, i.e., when the 2×2 reconstruction is well established and the adatom peak represents 16% of the segregated (second layer) Si peak. The binding energies and relative intensities of the components of the Si $2p$ line shape are summarized in Table I. The binding energy of the leading doublet in the as-deposited interface is 98.6 eV, i.e., the same energy shift with respect to the silicides as measured by Ebert and Panzner[26] for the saturated segregated surface of Fe–6 at. % Si.

The peaks shift to higher binding energy when the interface is annealed, and stabilize at 98.8 and 99.5 eV at 450–500 °C where the interface is α-$FeSi_2$-like. The intensity of the surface component is 50% of the total Si $2p$ signal, to be compared with the 33% of surface component measured on the polycrystalline α-$FeSi_2$ bulk phase. At this stage a 2×2 LEED pattern is observed, indicating a well-ordered, reconstructed surface. The

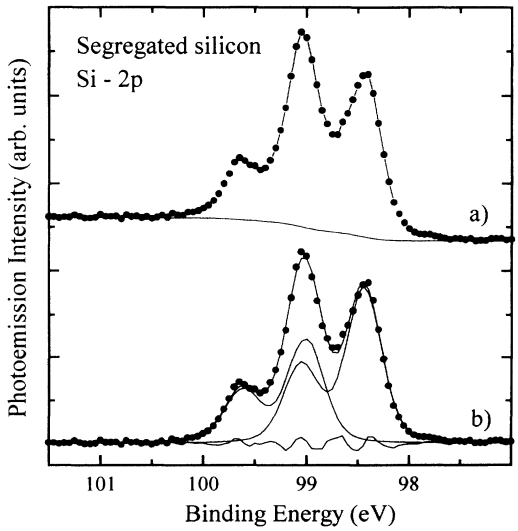

FIG. 9. Analysis of the segregated silicon Si $2p$ line shape on a polycrystalline iron surface: (a) raw data and integral background; (b) background subtracted data (points) and fitted line shape (continuous line) obtained with two doublets shifted by 0.57 eV. The bottom curve shows the residual of the fit.

reconstruction is due to silicon atoms terminating the silicide, or above the silicide termination layer, as seen in STM (Ref. 6) and in grazing incidence x-ray diffraction (GIXD).[7,14] According to a recent model,[14] the silicon adatoms can be in the $T4$ site, with a silicon atom directly below in the third plane, while iron atoms occupy most other third-layer sites. The second layer in this model is all silicon. This means that silicon segregation on iron silicides produces islands which are surface terminated by adatoms. When the size and ordering of the segregated islands increase, a long-range 2×2 network of adatoms becomes visible in the LEED.

At 600 °C a drastic change of the line shape occurs with the appearance of a peak at 99.1 eV, i.e., the substrate silicon peak. From the Fe $3p$ photoemission, we know that the β-$FeSi_2$ and α-$FeSi_2$ environments exist in a ratio 1:4. The same relative proportions of the Si $2p$ bulk silicide line shapes were used in the refinement of the integral Si $2p$ line shape at 600 °C. The resulting line shape obtained after the subtraction of the bulk silicide components is shown in the top of Fig. 8, where it is further decomposed in the two contributions of bulk silicon (continuous line) and surface segregated silicon. The latter presents the same line shape obtained for the lower temperatures. This is a clear sign of cracking of the silicide layer and agglomeration. It confirms the interpretation of the strong increase of the Si/Fe ratio in Fig. 1 for $T=600$ °C and higher as due to agglomeration, and not to decomposition of the silicide. Clear evidence of agglomeration is also provided by electron microscopy for similar interfaces.[7]

For annealing at higher temperatures the Si $2p$ line shape becomes progressively dominated by the substrate silicon, i.e., by the signal from increasingly uncovered portions of the substrate. The interface annealed at 750 °C presents both 7×7 and 2×2 LEED patterns. The line shape for this sample (curve a) is analyzed in Fig. 10. 60% of the intensity is attributed to 7×7 reconstructed regions of uncovered substrate (curve b). The remaining signal can be deconvoluted in equal amounts of bulk line shapes for α-$FeSi_2$ and β-$FeSi_2$ (curve c) and in two surface doublets at 99.2 and 98.6-eV binding energies (curve d). We attribute the doublet at 99.6 eV to surface segregation on the α-$FeSi_2$, corresponding to 1.5 ± 0.3 monolayers of silicon. Its 2×2 signal is mixed with the other components of the fit. The doublet at 99.2 eV is attributed to the surface segregation onto β-$FeSi_2$, corresponding to 1.7 ± 0.3 monolayers of silicon. By assuming a standard value of photoelectron escape depth at these kinetic energies (6 Å), identical for both silicon and silicides, we derive that about 30% of the substrate is covered with the interface silicides, which are in turn covered by silicon to a larger extent than the corresponding bulk phases. This interpretation is consistent with the electron microscopy and GIXD results that reveal the presence of β-$FeSi_2$ icebergs and the flat regions between the icebergs.[14] We suggest that the flat regions are in part due to uncovered silicon 7×7, and in part to islands of the α-$FeSi_2$-like phase, surface stabilized by the 2×2 reconstruction.

We summarize the steps undertaken in the analysis of the very complex Si $2p$ line shapes: the problem has been reduced by removing all of the contributions from silicide environments of silicon on the basis of the Fe-silicide core-level data, and by comparing the difference spectra to "standards" for uncovered Si(111)7×7 and for surface-segregated silicon on Fe. The 5% error bar on the relative bulk contributions is directly imported from the Fe $3p$ analysis. The relative amounts of the surface contributions are established by a fitting procedure well calibrated on clean Si(111)7×7 and segregated silicon standards. The main source of error stays within the determination of the relative amount of bulk and surface silicon intensities, which is of the order of 15%. We stress that a brute force curve fitting of the data with analytical line shapes could not yield stable and understandable results over the whole interface growth process. All the ingredients of the spectra reduction presented above are clearly necessary, since their intensities are much larger than the uncertainty of their relative proportions.

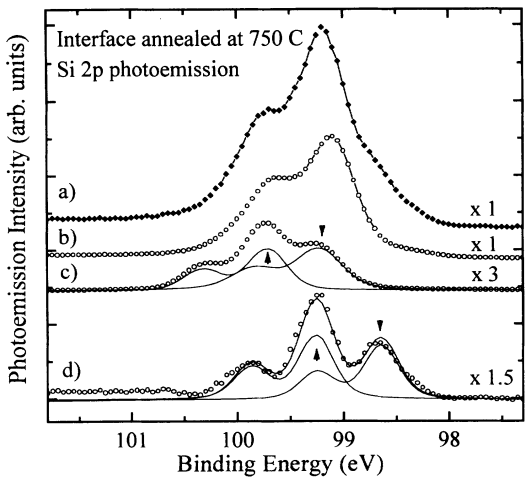

FIG. 10. Analysis of the Si $2p$ core-level photoemission (a) of the interface annealed at 750 °C; (b) Si(111)7×7 spectrum from the exposed substrate; (c) bulk silicide contributions from the α-$FeSi_2$ and β-$FeSi_2$ islands; (d) surface termination of the silicide islands. The higher-binding-energy bulk and surface components are due to β-$FeSi_2$ islands (up arrows); the lower-binding-energy silicide and surface components correspond to the α-$FeSi_2$ islands (down arrows).

Interface growth for 1.5×10^{15} Fe atoms/cm^2 on Si(111)7×7

The results for the thinner interface are fully consistent with those discussed above. Figure 11 shows the comparison of the Si $2p$ spectra obtained from the thinner interface as deposited and after annealing, with those obtained for the thicker interface at higher annealing temperatures. It is shown that the same line shapes (i.e., the same sequence of phases) are produced in both cases, but at lower temperature in the thinner interface. This confirms the interpretation of the temperature shift in Fig. 1 between the two coverages as a purely kinetic factor in the formation of the interface silicides.

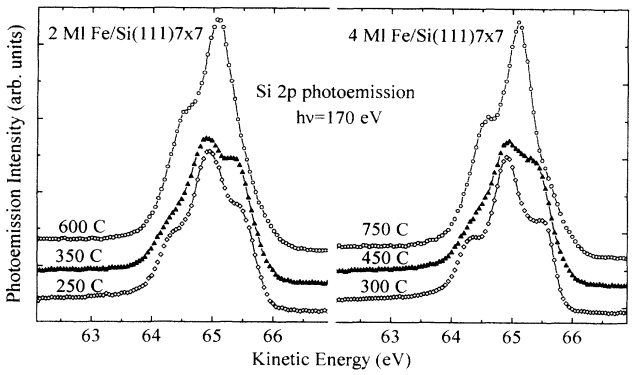

FIG. 11. Comparison between the Si $2p$ core-level photoemission spectra obtained after selected annealing temperatures for two different Fe deposits on the Si(111)7×7 surface: 2 and 4 ML.

Comparison with bulk phases

Much of the analysis of the present interface data has been carried out by comparing the line shapes with those of standard silicides. On this basis all of the results for Fe core levels and valence bands can be understood to represent the FeSi, α-$FeSi_2$, and β-$FeSi_2$ or combinations of silicides, i.e., FeSi+α-$FeSi_2$ at 300 °C and α-$FeSi_2$+β-$FeSi_2$ at temperatures of 600–750 °C. In particular, the interface disilicide which starts nucleating at 300 °C, forms a uniform layer at 400 °C and is stable up to the partial decomposition to β-$FeSi_2$ at 600 °C, is spectroscopically identical to bulk α-$FeSi_2$. As mentioned above, the core-level energy and line shape are very sensitive to the structure and density of states; in fact, in spite of a very similar nearest-neighbor environment, the Fe $3p$ photoemission peak of the α phase and β phase appear at 0.5-eV different kinetic energy due to the respectively metallic and semiconducting valence bands. Although the predicted γ-$FeSi_2$ phase is metallic and has a similar first-neighbor coordination, large differences from α-$FeSi_2$ occur in the Fe-Fe second-neighbor distances, which in the α phase occur at 2.68 Å for four neighbors and at 3.79 Å for the remaining four neighbors, while in the fluorite γ-$FeSi_2$ all eight Fe neighbors occur at 3.83 Å. This difference changes the Fe d-d interaction, perhaps the exchange splitting (zero in α-$FeSi_2$) and therefore the width of the $3d$ band; moreover it should be reflected in the core-level energies, line shapes, and satellites. The identity of valence-band and core-level spectra for the 400–500 °C annealed interface and bulk α-$FeSi_2$ uniquely identifies the interface silicide as an epitaxial α-$FeSi_2$ phase.

Surface termination of epitaxial silicides

The Si $2p$ core levels show surface features at all stages of the interface formation. The surface peaks of the as-deposited Fe layers are typical of segregation; in fact, similar energies are measured for Fe(100) 3 at. % Si, as well as polycrystalline Fe thick layers. The saturation of the segregated surface of a Fe(100) 6 at. % Si crystal[26] show a 2×2 pattern, indicating the tendency to form a broad lattice, low-density Si layer bonded to the substrate. The formation of cubic FeSi is accompanied by a 1×1 LEED pattern. At this stage the Si surface peaks shift to higher binding energy, and the adatom and subadatom peaks are roughly equal in intensity. The nucleation of the α-$FeSi_2$ phase stabilizes the 2×2 network, and the binding energy of the adatoms increases slightly.

The tendency to form 2×2 surfaces in the presence of Fe at the interface has been observed for a wide variety of cases, for submonolayer coverages where islands of only one plane of iron are formed,[6] and for MBE-grown cubic disilicides.[8] We observe that the binding energy for the surface silicon atoms is highest for the 2×2 on the α-$FeSi_2$ epitaxial phase, but that adatoms of the same nature are also present on the epitaxial FeSi and as surface-segregated atoms on any Fe-rich surface.

CONCLUSIONS

In summary, the solid-phase epitaxy of iron silicides in the ultrathin regime onto the Si(111)7×7 surface proceeds with the formation of a cubic FeSi epitaxial layer obtained for low-temperature annealing (200–300 °C) that is decomposed, starting at 300 °C into α-$FeSi_2$. The α-$FeSi_2$ layer is epitaxially ordered and its silicon termination is further stabilized by a 2×2 network of silicon adatoms. The interface α-$FeSi_2$ is a low-temperature stable phase fully commensurate with the Si(111) substrate, i.e., weakly strained [0.64% and −5.34% along the (100) and (001) directions], and different from the bulk α-$FeSi_2$ phase which is the high-temperature stable phase. Apart from this important difference, the electronic states of the interface α-$FeSi_2$ phase and the quenched-bulk α-$FeSi_2$ phase are identical within the accuracy of this experiment. The interface tetragonal α phase decomposes to the orthorhombic β-$FeSi_2$ phase starting at 600 °C. The surface in between the β-$FeSi_2$ islands is partially covered with two-dimensional (2D) rafts of the α-$FeSi_2$ phase with its 2×2 silicon surface capping. The rest is uncovered Si, reconstructed 7×7 after annealing at 750 °C. It is clear that the interface thermodynamics deeply influences the nucleation and decomposition of iron silicides. The irreversible sequence

$$\text{interface 2D } \alpha\text{-}FeSi_2 = 600\,^{\circ}\text{C} \Longrightarrow \text{3D } \beta\text{-}FeSi_2 \qquad (1)$$

is inverted with respect to the bulk reversible decomposition:

$$\beta\text{-}FeSi_2 \Longleftarrow 950\,^{\circ}\text{C} \Longrightarrow \alpha\text{-}FeSi_2\ . \qquad (2)$$

The better lattice match of the α phase with respect to the uniaxially strained match of the β phase onto Si(111)7×7 favors the formation of α-$FeSi_2$ up to a temperature where the highest bulk stability of β-$FeSi_2$ exceeds the cost of interface breaking and of agglomeration. Still at these low temperatures defects are needed to promote the decomposition (1) and in fact 2D rafts of the interface α phase are still found at the interface, along with 3D islands[7] of β-$FeSi_2$ for temperatures of 750 °C, i.e., much higher than the lowest observed decomposition

temperature (1). The present results complement the recent literature and unify the current knowledge of the SPE-grown silicides on Si(111)7×7. The interface stable disilicide is here recognized to be of the tetragonal α-$FeSi_2$ type. This is compatible with all LEED and STM observations, since a double cell of α-$FeSi_2$ is almost cubic and can be compared with the fluorite structure by condensing every second Fe plane in a single dense plane, leaving the same silicon positions. The α-$FeSi_2$ phase is also similar to the cubic CsCl structure of interface FeSi, and can be obtained from the latter by removing every second iron (001) plane, always leaving the same silicon positions. The evolution from the cubic CsCl-FeSi to the α-$FeSi_2$ can be understood as the removal of well defined Fe sites[14] rather than by the random substitution of Fe by Si, as proposed by the CsCl-$Fe_{1-x}Si$ model.[8] The fact that the Fe core levels are well explained by the coexistence of two bulklike phases is a strong support of this interpretation, rather than the continuous concentration gradient in the CsCl cubic silicide. We note that the SEXAFS (Ref. 15) results for the SPE-grown disilicide are fully compatible with the tetragonal structure, and can be interpreted as evidence of the α-$FeSi_2$ phase instead of a CsCl-type silicide. In addition, electron microscopy data[7] are nicely complemented by present results for the electronic properties of the icebergs and of the undefined 2D rafts, which we find for 2D α-$FeSi_2$. As a final remark, we suggest that the growth of interface silicides by SPE implies a reversal of the bulk nucleation and decomposition sequences, due to more favorable epitaxial growth for the α phase than for the β phase. But it does not provide evidence for extra metastable phases such as the γ-$FeSi_2$- or CsCl-type defect $FeSi_2$ that consequently can only be grown by MBE. Previous conclusions for the growth of fluorite γ-$FeSi_2$ by SPE on Si(111)7×7 based on submonolayer coverages[6] do not represent clear evidence, since if only one Fe plane is implied at the interface the only difference between $\gamma FeSi_2$ and α-$FeSi_2$ structures is a slight corrugation of the latter with respect to the former. Also the use of the 2×2 reconstruction as fingerprint for the γ-$FeSi_2$ phase is unjustified, since Si adatoms always exist at the surface of iron silicides and segregated silicon islands on iron and iron-rich films. The ordering in a 2×2 structure is obtained at least in the present case of α-$FeSi_2$ and at the surface of Fe(100) crystals.[26] We have also shown that Si adatoms always exist as surface stabilization of segregated silicon on iron single crystals and iron films as well as iron silicides.

ACKNOWLEDGMENTS

This work was partially supported by the Swiss National Fund under Program 24. Thanks are due to M. Sauvage-Simkin and A. Waldhauer for communicating their results to us prior to publication.

*Present address: Laboratoire de Cristallographie, CNRS, 25 Avenue des Martyrs, B.P. 166, Grenoble, France.

[1]H. von Känel, Mater. Sci. Rep. **8**, 193 (1990).

[2]J. Derrien, J. Chevrier, V. Le Than, and J. Mahan, Appl. Surf. Sci. **56/58**, 382 (1992).

[3]M. deCrescenzi, G. Gaggiotti, N. Motta, F. Patella, and A. Balzarotti, Phys. Rev. B **42**, 5871 (1990); J. Derrien, J. Chevrier, V. Le Thanh, T. E. Crumbaker, J. Y. Natoli, and I. Berbezier, Appl. Surf. Sci. **70/71**, 546 (1993).

[4]N. E. Christensen, Phys. Rev. B **42**, 7148 (1990).

[5]H. von Känel, R. Stalder, H. Sirringhaus, N. Onda, and J. Henz, Appl. Surf. Sci. **56-58**, 196 (1992); J. Chevrier, V. Le Thanh, S. Nitsche, and J. Derrien, Appl. Surf. Sci. **56-58**, 438 (1992).

[6]A. L. Vasquez de Parga, J. de la Figuera, C. Ocal, and R. Miranda, Europhys. Lett. **18**, 595 (1992).

[7]N. Jedrecy, Y. Zheng, A. Waldhauer, M. Sauvage-Simkin, and R. Pinchaux, Phys. Rev. B **48**, 8801 (1993), and references quoted therein.

[8]H. von Känel, K. A. Mäder, E. Müller, N. Onda, and H. Sirringhaus, Phys. Rev. B **45**, 13 807 (1992); H. Sirringhaus, N. Onda, E. Müller-Gubler, P. Müller, R. Stalder, and H. von Kanel, *ibid.* **47**, 10 567 (1993).

[9]V. Le Thanh, J. Chevrier, and J. Derrien, Phys. Rev. B **46**, 15 946 (1992).

[10]Y. Desausoy, J. Protas, R. Wandji and B. Roques, Acta Crystallogr. B **27**, 1209 (1971).

[11]J. Chevrier, P. Stocker, V. Le Thanh, J. M. Gay, and J. Derrien, Europhys. Lett. **22**, 449 (1993).

[12]Y. L. Gavriljuk, L. Y. Kachanova, and V. G. Lifshits, Surf. Sci. Lett. **256**, L589 (1991).

[13]W. Raunau, H. Niehus, T. Schilling, and G. Comsa, Surf. Sci. **286**, 203 (1993).

[14]M. Sauvage-Simkin, N. Jedrecy, A. Waldhauer, and R. Pinchaux, in *Proceedings of the Third International Conference on Surface X-rays and Neutron Scattering, Dubna (Russia), 1993* [Physica B (to be published)]; A. Waldhauer, PhD. thesis, University, Paris, 1993.

[15]U. Kafader, M. H. Tuilier, C. Pirri, P. Wetzel, G. Gewinner, D. Bolmont, O. Heckmann, D. Chandesris, and H. Magnan, Europhys. Lett. **22**, 529 (1993).

[16]X. Wallart, H. S. Zeng, J. P. Nys, and G. Dalmai, Appl. Surf. Sci. **56-58**, 427 (1992).

[17]Y. Ufuktepe and M. Onellion, Solid State Commun. **76**, 191 (1990).

[18]J. Alvarez, J. J. Hinarejos, E. G. Michel, and R. Miranda, Surf. Sci. **287/288**, 490 (1993).

[19]F. Sirotti, M. DeSantis, and G. Rossi, Phys. Rev. B **48**, 8299 (1993).

[20]F. Sirotti, M. DeSantis, Xiaofeng Jin, and G. Rossi, Appl. Surf. Sci. **65/66**, 800 (1993).

[21]J. J. Yeh and I. Lindau, At. Data Nucl. Data Tables **32**, 34 (1985); **32**, 46 (1985).

[22]B. T. Thole and G. van der Laan, Phys. Rev. B **38**, 3158 (1988).

[23]S. Doniach and M. Sunjic, J. Phys. C **3**, 285 (1970).

[24]C. Carbone, J. Kachel, R. Rochow, and W. Gaudat, Z. Phys. B **79**, 325 (1990); F. U. Hillebrecht, R. Jungblut, and E. Kisker, Phys. Rev. Lett. **65**, 2450 (1990).

[25]J. F. van Acker, Z. M. Stadnik, J. C. Fuggle, H. Hoekstra, K. Bushow, and G. Stroink, Phys. Rev. B **37**, 6827 (1988).

[26]B. Egert and G. Panzner, Phys. Rev. B **29**, 2091 (1984).